Induced Master Motion in Force-Reflecting Teleoperation

Katherine J. Kuchenbecker and Günter Niemeyer
Telerobotics Lab
Mechanical Engineering Department
Stanford University
http://telerobotics.stanford.edu
{katherine.kuchenbecker, gunter.niemeyer}@stanford.edu

***Abstract*— Telerobotic systems have persistently struggled to provide users with realistic force feedback; high-frequency contact transients convey important information about the remote environment but are typically attenuated to avoid the contact instability they incite. This undesirable behavior can be traced to induced master motion, movement of the master device that is caused by force feedback rather than user intention. Such motion is interpreted as a position command to the slave, closing an internal control loop that is unstable under high gain. This paper examines the phenomenon of induced master motion in position-force teleoperation, presenting a new approach for achieving stable, high-gain force reflection using model-based cancellation. Requirements for the model of the induced motion dynamics and methods for its characterization are described, focusing on successive isolation of inertial and connecting elements. The sixth-order nonlinear model obtained for a one-degree-of-freedom user-master system is validated and then tested in a cancellation controller. Canceling induced master motion during teleoperation is shown to improve the stability of impacts, allowing significantly higher force reflection levels and a more authentic user experience.**

I. Introduction

Teleoperation has long pursued the goal of remote manipulation, promising users the ability to interact naturally with environments that are normally beyond human reach. The first such systems were developed in the late 1940s to let an operator handle radioactive materials from behind a shielded wall [1]. These early master and slave robots were connected mechanically and behaved as a single extended tool. The user could easily feel interaction forces from the remote environment as they were transmitted directly through the mechanism. The applicability of such systems was greatly increased by replacing their simple mechanical connection with an electric control system [2]. At present, humans use telerobotics to explore the deep sea, assemble equipment in space, and perform minimally invasive surgery; unfortunately, these modern systems all struggle to provide the user with natural-feeling force feedback.

An ideal teleoperator would make remote interactions feel like direct manipulation, portraying the dynamics of the distant environment without distorting the user's motions or haptic perceptions. Normal human hand movements contain frequencies up to a few Hertz, which most telerobotic systems can easily track. Teleoperators encounter far more difficulty in providing good haptic feedback; in contrast to the low-bandwidth of human actuation, humans can sense forces from DC up to a kilohertz. Particularly important are the high-frequency transient signals caused by contact between a tool and a hard object, a nonlinear phenomenon [3]. Humans can process these short-duration reaction forces, which often resemble decaying sinusoids, to determine the material and geometry of the object being touched. Research has shown that portraying such signals increases the dexterity and realism of haptic interactions [4]–[7], but present telerobotic systems can seldom convey such nuanced force feedback.

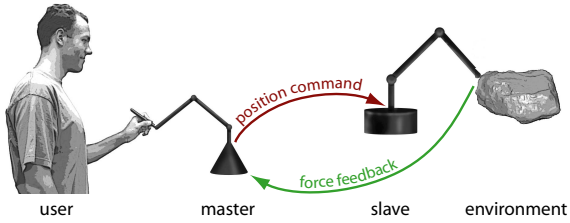

Fig. 1. A telerobotic system connects the user to the environment via master and slave robots.

Among the many controllers used in telerobotics, the position-force architecture seeks to provide accurate feedback by explicitly measuring the force of contact between the slave and the environment. As illustrated in Fig. 1, the slave is commanded to follow the measured position of the master mechanism. Forces sensed at the slave are simultaneously displayed via the master's motors, transmitted to the user's hand via the structure of the device. One fascinating aspect of this architecture is as follows: throughout an interaction, the master mechanism must perform the dual tasks of position measurement and force display. The master's dynamics couple these two functions together, allowing the device's force output to affect its position input. Like a sound system whose microphone is too close to the speakers, telerobotic systems let high-frequency force feedback induce motion of the master device that is then treated as a position command. During environment contact, this induced motion can drive the entire system unstable with high-frequency vibrations, similar to the screeching of a badly configured sound system. As with speaker volume, the force feedback gain must usually

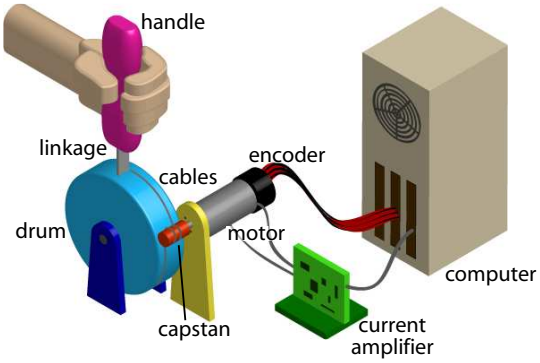

Fig. 2. The master's long dynamic chain connects the user to the controller.

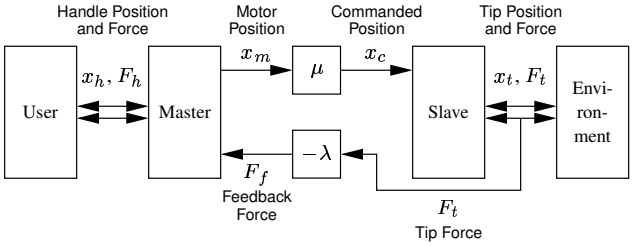

Fig. 3. In position-force control, the slave is commanded to track the master's position, and the master mechanism recreates tip interaction forces for the user.

be lowered to achieve stability, reducing haptic cues to the user and leaving interactions feeling soft and ill-defined.

This work explores the phenomenon of induced master motion, the common culprit of instability in force-reflecting teleoperation. We begin by providing a technical framework in Sec. II, formally defining the problem in Sec. III, and reviewing previous approaches in Sec. IV. The induced master motion viewpoint inspires a new control methodology for stabilizing high-gain force reflection, the approach of model-based cancellation of induced master motion, which is described in Sec. V. The requirements for an induced master motion model are discussed in Sec. VI, and Sec. VII describes appropriate system identification strategies. In Sec. VIII, we present the model we obtained for a one-degree-of-freedom (one-dof) user-master system and demonstrate its cancellation performance during teleoperation. Sec. IX summarizes our findings and suggests avenues for future work.

II. Telerobotics Framework

To facilitate an analysis of induced master motion, we first describe the primary components of a standard master device and specify the relevant controller architecture.

A. Typical Master Hardware

A telerobotic master performs the two main tasks of measuring the motion of and applying forces to the user's hand. This research is concerned with impedance-type devices, wherein the entire mechanism is back-drivable to allow easy free-space motion. Despite its prominent role of connecting the user to the controller, remarkably little research has explored the master's influence on overall system behavior. Today's telerobotic systems usually provide two or three degrees of freedom in position, and Fig. 2 illustrates the chain of elements typically present in each axis of the master. Although differences exist, individual axes of most mechanisms can be represented by such an arrangement.

The controller runs on a real-time enabled computer at a fixed servo rate, often one kilohertz. Feedback forces are converted to a desired current for each DC motor, and this command is communicated to a self-contained amplifier that regulates motor current via pulse width modulation or linear control techniques. Current flowing through the motor creates a torque on the motor shaft, to which a small capstan is attached. Thin stranded cables couple motion of the capstan to that of a larger drum, amplifying the torque produced by the motor by a factor of ten to twenty. The drum is attached to the endpoint of the device through a mechanical linkage that is often somewhat flexible, and the user holds a handle, stylus, or thimble at the endpoint. Such devices are designed with low friction and low inertia to allow the user to easily move them around. Motion of the master is usually sensed with an optical encoder located on the motor shaft, providing a discrete position signal to the controller. For the duration of this paper, the term "master" will stand for all electrical and mechanical elements depicted in Fig. 2, extending from the amplifier and motor to the handle.

B. Position-Force Control

Telerobotic systems often use position-force control to allow the user to feel the slave robot's contact with the environment. A standard position-force architecture is illustrated in Fig. 3, showing user, master, slave, and environment. During teleoperation, the user holds the handle of the master mechanism and moves it around. Assuming a causality for this interface is not required for our work, so we simply depict the interaction with two double-headed arrows. The system monitors the position of the master mechanism's motors, x_m, and commands the slave robot to move accordingly via x_c. The slave controller attempts to make the slave track this motion command, typically via proportional, integral, and/or derivative control. We draw the interaction between the tip of the slave arm and the environment as bidirectional in position and force, again to avoid an unnecessary assumption of causality.

As the slave moves around, the system captures the effects of environmental contact by measuring the force exerted by the tip, F_t. Mounting the force sensor at the slave's end-effector highlights contact dynamics and masks the robot's internal friction and inertia. Such an arrangement is particularly important for capturing the forces that stem from nonlinear events such as impacts. To let the user feel how the interaction is progressing, the measured tip force is continuously displayed via the motors on the master device as F_f.

The forward position scaling ratio, μ, and the force feedback gain, $-\lambda$, can be used to adjust the interaction between the two sites [8], following the naming convention of Daniel and McAree [9]. Typically, μ is chosen to scale comfortable human hand movements to the workspace of the slave robot, allowing

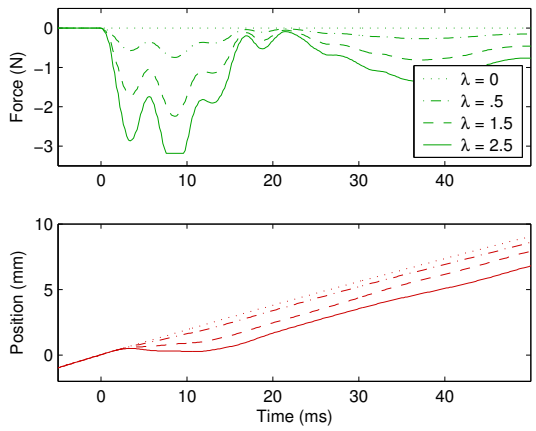

Fig. 4. Display of a scaled, pre-recorded force profile to a user executing a constant motion. Increasing the force scale λ generates motor movement that is not intended by the user.

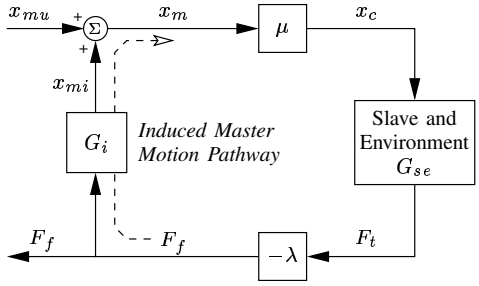

Fig. 5. Motion induced by the force feedback, x_{mi}, superimposes with motion intended by the user, x_{mu}, at the master motor. The passive dynamics of the user-master system, G_i, govern the pathway of induced master motion.

the user to perform the chosen task as though it were a familiar manual manipulation. Common values of μ include 0.004 for nanomanipulation [10], about 0.33 for minimally invasive surgery [11], and 10 for industrial assembly.

Once μ is selected, an appropriate value for λ must be found. In the same way that human motion is scaled to match the task, contact forces should be scaled up or down to match human sensory capabilities [12]. Human users want to comfortably feel the slave's interaction with the environment. Unfortunately, stability concerns usually limit the force reflection ratio to values below this desired level [13]. In practice, λ is selected by gradually increasing it from zero until the slave begins exhibiting contact instability, unnatural vibrations when touching hard objects. At this relatively low value of λ, soft objects are generally difficult for the user to detect, and hard objects feel like foam or rubber rather than wood or metal. Systems that can support higher values of λ for a given μ will provide stronger haptic cues to the user, allowing more natural interactions and greater sensitivity during delicate operations such as microsurgery. Although the perspective of induced master motion is applicable for any position scale, the remainder of this paper will choose $\mu = 1$ for simplicity and attempt to increase λ.

III. Induced Master Motion Pathway

When employing a typical master device in position-force control, one encounters a maximum force feedback gain λ, above which the system cannot make stable contact with hard objects in the environment. This behavior can be understood by carefully examining the effect of the master dynamics on the controller. As seen in Fig. 2, the master connects the user to the controller via a series of dynamic elements. The user's hand acts on the master at the handle, via x_h and F_h, while the controller applies a force at the motor, F_f. These two interfaces jointly determine the movement of the device, driving the position of the master motor, x_m.

In the absence of force feedback, the human is the only active influence on the master, and x_m is a good measurement of his or her smooth, low-frequency hand motion. When the controller applies additional forces at the motor, these forces interact with the dynamics of the user-master system and cause movement that the human did not intend. To illustrate this phenomenon, Fig. 4 shows the first fifty milliseconds of measured motor motion during open-loop force display on a one-dof master. The user moved the handle of the device at a constant velocity, and a scaled, pre-recorded force profile was displayed when the motor crossed a position threshold. The dynamic coupling between force feedback and motor position is visible as sudden deviations from the user's smooth, $\lambda = 0$ path, happening far faster than the human's cognitive reaction to the applied force, which takes approximately 100 ms. Higher levels of force reflection provide stronger haptic cues to the user but also cause more significant divergence from the user's smooth, intended path. We call these deviations *induced master motion* because they stem from the force feedback signal rather than from the user.

In a full telerobotic system, the controller uses the master motor position as an indication of the user's intentional hand movement, forming the slave command x_c as μx_m. Systems that do not provide force feedback can trust x_m to reflect the user's intended hand motion. In this case of $\lambda = 0$, the slave can make stable contact with the environment, but the user must rely on visual cues to judge the progress of the interaction. When λ is increased above zero, the applied force feedback directly corrupts the controller's measurement of user motion by changing the motor's path. As seen in Fig. 4, higher force reflection ratios induce more motion of the master motor.

The measured position of the master, x_m, is determined both by the user's active influence on the handle and by the system's passive response to the feedback forces applied at the motor [9], [14]. Recognizing the low-frequency nature of human movement, we approximate this relationship via superposition and write

$$x_m(t) = x_{mu}(t) + x_{mi}(t), \tag{1}$$

where x_{mu} is the user's active contribution, x_{mi} is induced by force feedback, and t is time. Furthermore, we define the connection from force feedback to unintentional motor movement as

$$x_{mi}(t) = G_i\left(F_f(t)\right), \tag{2}$$

where G_i represents the induced motion dynamics of the user-master system. This function depends on electrical and

mechanical characteristics of the device and on the instantaneous biomechanical properties of the user. This treatment of induced master motion is illustrated in the block diagram of Fig. 5, lumping the slave and environment into one element. We leave out the user's perception of the feedback force and his or her generation of intentional motor motion because the representation of such cognitive processes is beyond the scope of this research. It is worthwhile to note, though, that our assumption of superposition is consistent with the common linear user model of a spring and damper connected to a slowly changing desired position [9].

During teleoperation, the pathway of induced master motion interacts with slave and environment dynamics to form an internal controller loop that includes both μ and λ, as can be seen in Fig. 5. From this diagram, we can write out the equation for x_m, proceeding once around the loop:

$$x_m(t) = x_{mu}(t) + G_i\left(-\lambda G_{se}\left(\mu x_m(t)\right)\right). \tag{3}$$

The physical interpretation of this signal loop is that the natural dynamics of the user-master system, G_i, allow the controller's force feedback signal to induce master motion and thus directly influence the slave's position command. Slave contact with stiff objects causes large force transients, which induce significant master motion. This induced motion is interpreted as a slave movement command, which causes tip motion and additional force feedback from the environment. Under assumptions of linearity and time invariance, (3) yields the loop's transfer function and characteristic equation.

For a given position scale, there generally exists a force feedback gain above which a position-force controlled system cannot maintain stable contact with stiff objects. Daniel and McAree use conservation of momentum to show that an uncompensated position-force system must keep the product of μ and λ less than or equal to m_m/m_s to be stable, where m_m and m_s are the effective masses of master and slave respectively [9]. Although a detailed derivation of the general case is beyond the scope of this paper, we assert that this threshold is determined by the dynamic interaction between the induced master motion pathway, G_i, and the slave-environment system, G_{se}. Widely observed in practice, the slave enters a limit cycle at high values of λ, repeatedly making and breaking contact with the environment. In addition, moderate values of λ for a given μ prolong the contact transient, distorting the environment's response. Lowering the force reflection ratio re-establishes functional operation but gives the user only a limited ability to discern environment properties. Ideally, user preference and task requirements would guide selection of λ, rather than stability.

Little research acknowledges the pivotal role that the passive dynamics of the user-master system play in this limitation. Identifying the actual relationship between F_f and x_{mi} can contribute to an understanding of overall system behavior, including a derivation of the stability threshold. Masters can be evaluated according to the G_i they provide, as systems that permit less induced master motion will support the higher force feedback levels that are commonly desired. Furthermore, the electrical and mechanical components of existing master systems can be modified to adjust G_i and increase the force-feedback gain that they will stably support. In summary, induced master motion compromises the stability of a telerobot by allowing the force feedback signal to influence the slave's commanded position, creating an internal control loop that is unstable under high gain.

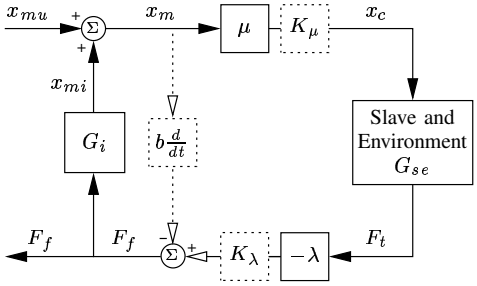

Fig. 6. Position-force control with three compensation options: local derivative feedback on master position via $b\frac{d}{dt}$, position command filter K_μ, and force feedback filter K_λ.

IV. Prior Approaches

Recognizing that teleoperative contact instability occurs when the force-feedback gain λ is too large for a given position scale μ, many researchers have proposed strategies for handling this trade-off. As mentioned above, the simplest approach lowers the force feedback gain until contact with the stiffest environment elements becomes stable. Such a choice reduces the intensity of the user's force cues and often leaves lightly damped oscillations that can distract from the interaction. Another basic tactic requires the user to hold the master mechanism with a firmer grasp or even with two hands. Increasing the user's impedance in such a way attenuates handle motion and generally decreases induced motor motion, lowering the magnitude of G_i. A firmer user grasp can quell some marginally unstable oscillations, but it is not a solution to the underlying problem.

More sophisticated methods are required to overcome the instability generated by position-force control. Many proposed strategies aim to accomplish this goal by shaping the signals of the system's internal feedback loop. Three standard stabilization approaches are illustrated in Fig. 6, including local derivative feedback on the master, a position-command filter, and a feedback-force filter. These modifications can be used alone or in tandem to adjust the behavior of a troublesome system, as discussed below.

The first illustrated approach for suppressing induced master movement is to add damping to the master manipulator via local feedback [15], [16]. Augmenting the block diagram with negative derivative feedback from x_m to F_f changes the system's loop relationship to

$$x_m(t) = x_{mu}(t) + G_i\left(-b\,\dot{x}_m(t) - \lambda\, G_{se}\left(\mu\, x_m(t)\right)\right). \tag{4}$$

The added term punishes high motor velocities via an opposing control force, which is added to the force feedback signal before being applied to the motor. Although it can stabilize contact, this additional damping is also apparent to the user

and makes the system feel slow and unresponsive, even when the slave is moving in free space. Furthermore, this strategy requires a clean, accurate measurement of velocity, which is seldom available in systems that rely on numerical differentiation of discrete position signals.

Other researchers have explored the possibility of putting a compensator in the slave's commanded position via K_μ [14]. The loop equation then becomes

$$x_m(t) = x_{mu}(t) + G_i\left(-\lambda\, G_{se}\left(K_\mu(\mu\, x_m(t))\right)\right). \quad (5)$$

When K_μ is a low-pass or notch filter, it attenuates the position command's destabilizing frequency content, but it can also prevent the slave from tracking quick movements by the user. In the general case, the compensator must be carefully selected to avoid adding too much lag at the crossover frequency, which would compromise the system's stability margins.

The third main stabilization strategy involves low-pass or notch filtering the force feedback signal via K_λ, removing mid- to high-frequency content before display on the master mechanism [9], [17]. This compensator yields

$$x_m(t) = x_{mu}(t) + G_i\left(K_\lambda\left(-\lambda\, G_{se}\left(\mu\, x_m(t)\right)\right)\right). \quad (6)$$

Filtering the force feedback can stabilize a system, but it also prevents the user from feeling any high-frequency signals, resulting in interactions that feel soft and undefined. Such a choice enables stability under higher force reflection ratios, but it compromises the information content of the feedback signal, especially when initiating contact with a stiff environment.

The feel of a system with filtered force feedback can be improved by using a separate actuator to display the signals removed by K_λ, a technique often described as combined vibrotactile and force feedback [4]. This frequency-domain separation increases the information available to the user while maintaining system stability. It should be noted that the vibrations from the additional actuator must be carefully isolated from the forward position command so that they do not enter the closed loop and incite contact instability. This strategy of combining actuators effectively bypasses the pathway of high-frequency induced master motion, staving off instability while allowing the user to feel a fuller spectrum of environment feedback.

V. Cancellation Approach

As an alternative to standard loop-shaping strategies and additional actuators, we can use the perspective of induced master motion to break the internal loop of the controller via model-based cancellation. First proposed in [18], the cancellation approach centers on understanding the passive response of the user-master system during a telerobotic interaction. As illustrated in Fig. 7, force feedback induces deviations from the user's intended path through the element G_i. We model the relationship between F_f and x_{mi} as $\hat{G}_i$ and use it to cancel induced master motion via real-time simulation. The model's response, $\hat{x}_{mi}$, is subtracted from the measured master position, x_m, to provide an estimate of the user's intended path, $\hat{x}_{mu}$. This estimate is multiplied by μ to become the slave's position command, x_c, providing a signal that

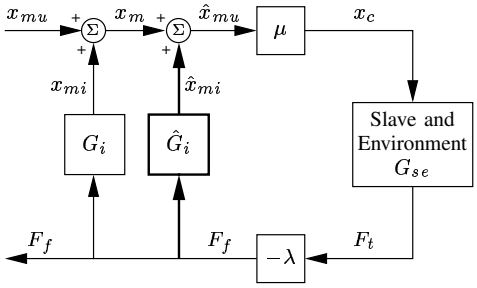

Fig. 7. Induced master motion can be canceled using the model $\hat{G}_i$.

is ideally free from feedback artifacts. For a treatment of our cancellation approach in the commonly used four-channel architecture for teleoperation, please see the Appendix.

Although new in telerobotics, canceling induced master motion bears a resemblance to several existing model-based control strategies. Some researchers attempt to hide the dynamics of the master from the user to make it feel like a weightless bar rather than a physical device [19], [20]. Typically modeling the master as a simple mass with viscous damping, they apply additional feedback forces to cancel the inertial and frictional forces estimated from position measurements. Another application of model-based cancellation is biodynamic feedthrough, where accelerations of a mobile vehicle apply forces to the body of the operator and therefore to the on-board control joystick. With a simple, second-order model of these dynamics, one can apply equal and opposite torques to the joystick and avoid instability [21], [22]. We extend these force-canceling ideas to cancellation of induced master motion, where we want the operator to feel the applied feedback without allowing the forces to affect the slave's position command.

The key element to this approach is obtaining a good model, $\hat{G}_i$, which will be the subject of the next two sections. The model must capture the response of the master motor to force feedback as a user holds the device's handle. With cancellation in place, the system's loop relationship becomes

$$\hat{x}_{mu}(t) = x_{mu}(t) + G_i\left(-\lambda\, G_{se}\left(\mu\, \hat{x}_{mu}(t)\right)\right) - \hat{G}_i\left(-\lambda\, G_{se}\left(\mu\, \hat{x}_{mu}(t)\right)\right). \quad (7)$$

The more closely the model approximates real system behavior, the more attenuated the connection from F_f to x_c becomes, stabilizing the system for higher force-feedback gains. Even a rough approximation of the system's high-frequency response under the conditions that incite instability will reduce the controller's loop gain and stabilize contact for moderate values of λ. The user will be able to feel strong feedback forces, and the slave command will closely approximate the path that the master motor would have taken in the absence of force feedback.

VI. Modeling User-Master Dynamics

To achieve the benefits of the cancellation approach, one must obtain a good model of the relationship between force feedback and induced motor movement; denoted $\hat{G}_i$, this

model of the user-master system need not be linear or time-invariant. As illustrated in Fig. 2, the target system extends from the master's amplifier and motor through its cables, drum, linkage, and handle to the user's hand and arm. The common model for these dynamics is a single mass connected to ground by a linear spring and damper; although second-order models perform well in other applications, the relevant dynamics of this complex system and the performance requirements for cancellation control must be closely examined before selecting an induced motion model.

A cancellation controller will use the model $\hat{G}_i$ for real-time simulation during telerobotic interactions. We thus evaluate a particular model by its ability to capture motor movement under force feedback as a user attempts to hold the handle still, following the superposition assumption from Sec. III. We test the model using force transients recorded from contact between the system's slave and environment. These signals contain frequencies from DC up to many hundreds of Hertz, depending on the combined bandwidth of the tip-mounted force sensor and the feedback filter K_λ, if used. We analyze model fidelity for a wide range of λ values, applying forces up to the maximum level that the master motor can generate. The importance of the system's response to these large-magnitude, high-frequency transients emphasizes the need to consider higher-order models, as internal master dynamics can create high-frequency resonances that strongly affect the induced motion response.

While device dynamics are considered constant, the user's influence on the system varies over time. Each user's hand dynamics are unique, and the connection between hand and handle will naturally change with grip force and arm muscle co-contraction. To account for these biodynamics in the model, a time-varying spring-like element can be placed between ground and the mass of the handle. Many researchers use spring-damper models to describe passive biodynamics [23]–[25], and our previous investigations have supported the efficacy of such a user model in haptic interactions [18], [26]. The element's properties can be linked to an indication of the user's effective impedance such as a grip force measurement [27], [28] or an EMG reading [29], [30]. Most likely, the relationship between the sensed quantity and the hand's dynamic behavior will need to be calibrated for each user [26]. We can use a general time-invariant model only if variations in the user's dynamics are relatively small, such as if we require the human to maintain a comfortable grip on the handle.

In addition to his or her passive biodynamic influence on the master system, the user can actively respond to low-frequency feedback signals. At low frequency, the entire master moves as one object, pushing back against the user's hand when the slave sustains contact with an obstacle. The user's arm and the master's structure do naturally deflect under such loads, but these deflections do not affect the user's ability to control the slave position under visual feedback. Effectively, the user removes low-frequency induced motion from the slave command via active compensation, applying additional hand forces and adjusting hand position at frequencies from steady state to about 5 Hz. To avoid interfering with this normal, stable process, the model used in a cancellation controller must significantly underestimate low-frequency induced motion while preserving accurate behavior at high frequency. As seen in (7), overestimating the total response of the user-master system creates positive feedback, which can destabilize the control loop and should be avoided. With these requirements in mind, we now describe techniques for obtaining an appropriate model of the user-master system, one that captures the high-frequency induced motion response while drastically underestimating steady-state deflections.

VII. System Identification

The relationship between force feedback command, F_f, and measured master motor position, x_m, depends to some extent on all of the elements in the long chain connecting the user to the controller. The objective of the system identification process is to determine the most important effects and include them in the model $\hat{G}_i$. This model is constructed around translation of the user's hand, converting torques and rotations to their effective values in this space. We begin by investigating the system's behavior as a whole, and then we dissect it to obtain physically-based parameters via our technique of successive isolation. At each step in the process, carefully chosen force commands are applied to the master, and the resulting motor movement is measured. Commands and measurements must be executed with very consistent timing, using a fast servo rate of a few kilohertz on the control computer.

A. Comprehensive Evaluation

Examining the overall induced master motion response, G_i, reveals the complexity of the underlying system. We have found non-parametric methods known as black-box modeling to be well suited for this task [18], [26]. With the user holding the master's handle in a comfortable grip, a swept-sine-wave force signal varying from several hundred Hertz to about one Hertz is commanded. An empirical transfer function estimate (ETFE) can then be formed by dividing the discrete Fourier transform (DFT) of the position output by that of the force input. To reduce the effects of sensor discretization and low-frequency human movement, the ETFEs from several tests are averaged together in the complex domain, and the resulting magnitude and phase values can be smoothed using a boxcar filter. The results can be treated as an experimentally determined Bode plot, providing insight into the system's dynamic behavior.

Performing the above procedure at a variety of signal magnitudes, frequency ranges, positions in the master workspace, and user grip force levels will elucidate the linearity of the system's behavior. If the experimental Bode plots match closely for a variety of conditions, the master's mechanical dynamics can be modeled as independent from such changes. Ideally, all of the comprehensive ETFEs would match, and a simple second- or fourth-order linear model could be tuned to match the total observed behavior. The model's time-domain response would then need to be validated for a set of typical force transients, and the parameters would need to be adjusted to underestimate by approximately one order of magnitude at very low frequency. More commonly, the

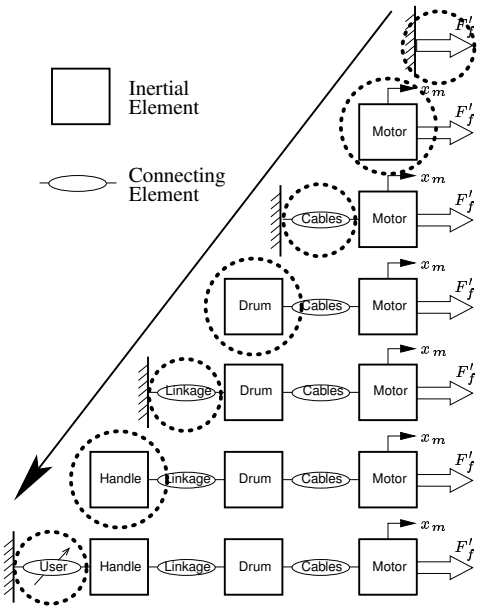

Fig. 8. Successive isolation of the user-master system progresses from the force command through the motor, cables, drum, linkage, handle, and user.

comprehensive ETFEs generated under various conditions do not match well and/or do not correspond to an easily deduced linear system. In these cases, building a model step by step from the physical system can help us thoroughly understand its behavior, separating out higher-order dynamics, nonlinearities, and the influence of the user.

B. Successive Isolation

An accurate induced motion model can be obtained by identifying each of the master's many dynamic elements in turn, as originally proposed in [31]. Such an approach yields a model whose parameters have physical significance, facilitating the addition of a varying user element and informing the device design process. We begin by separating the system's dynamic chain into alternating inertial and connecting elements, as illustrated in the bottom row of Fig. 8. We then proceed to identify each element's properties in turn, mechanically breaking the dynamic chain at points progressively farther away from the force input and position output. At each stage, we conduct quasi-static and dynamic tests, comparing observed and modeled behavior in both the frequency and time domains; only the model's outermost parameters are adjusted to make its response match our observations.

The first dynamic element to consider is the current amplifier, which is commonly assumed to be ideal. Amplifiers often effectively low-pass filter the commanded force and can add other important effects to the system's behavior. Particular attention should be paid to steady-state gain, offset, linearity, saturation, frequency response, and back-EMF rejection. Tests should be conducted both with the motor immobilized and with it spinning freely, measuring the actual current in real time as appropriate wave forms are commanded, While F_f is the commanded force, we define F'_f to be the force actually applied to the system by the amplifier.

Next we start the process of adding inertial and connecting elements in order, working away from the amplifier. When an inertial element is appended to the dynamic chain, the connecting element beyond it must be disengaged so that the mass can move freely; for example, when the motor is added, the cables must be disconnected. We then seek to determine the new element's inertia and dissipation parameters. Although dynamic models typically include only viscous friction, Coulomb friction is the dominant dissipator in haptic devices [32] and should be characterized in models of induced master motion. Coulomb friction is commonly found at sliding interfaces, and its effect is characterized by linear, rather than exponential, decay of transient dynamics. Coulomb friction can be determined by measuring the force required to move the present set of system elements across the workspace under closed-loop position control. Inertia and viscous friction can be highlighted by adding a virtual spring to the motor's end of the chain and analyzing both the frequency and time response of the resulting system. When identifying inertial elements, open-loop experiments that do not include a virtual grounding force should generally be avoided; the unconstrained movements that result are very sensitive to initial conditions and are not representative of the high-frequency oscillatory behavior that we wish to understand.

The focus advances to the next connecting element once an inertial element's parameters are estimated and validated. The connector should be attached to its neighboring masses, and the distant mass should be immobilized mechanically; for example, when the cables are first added to the system, the drum's position should be locked. The important characteristics for each connecting element are its possibly nonlinear stiffness and its dissipation. Although dynamic models commonly include only linear springs, large deflections of most physical objects reveal nonlinear relationships between position and force as well as occasional hysteresis. The stiffness of a connecting element can be examined by slowly varying the motor force and measuring the resulting position variations. Non-constant slope can be appropriately parametrized, and hysteresis can be modeled with a simple method we presented in [31]. The link's properties can also be highlighted using the ETFE method presented above, and its overall behavior can be validated via time response. When a connection is fully characterized, the inertial element beyond it is added to the chain and the successive isolation process continues.

VIII. Experimental Results

The modeling and control techniques presented in this paper were developed through implementation on a one-dof telerobotic testbed. The system's master and slave are a pair of Impulse Engine 2000's, high-quality force-feedback joysticks produced by Immersion Corporation. As shown in Fig. 9, the forward-backward axis of each device includes a DC motor connected to the handle via a cable drive, drum, and mechanical linkage. The rectangular joystick bases contain the motors and their respective current amplifiers. An ATI Mini40 force sensor is located beneath the front transmission element of the slave joystick so that the contact force between

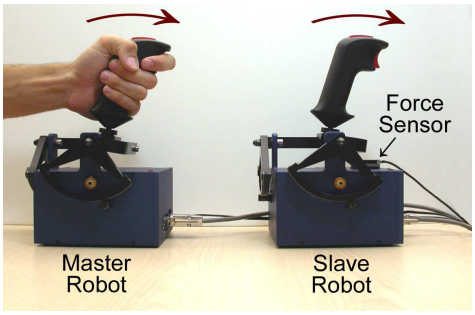

Fig. 9. Single-axis position-force telerobotic testbed.

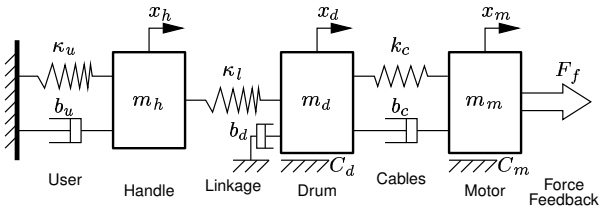

Fig. 10. Nonlinear lumped-parameter model of the user-master system. The κ parameters signify nonlinear stiffness relationships, and the C parameters indicate Coulomb friction.

it and the slave can be measured throughout an interaction. The hardware is controlled by a desktop computer running RTAI Linux, a hard-real-time open-source operating system, and all device control software was written in C. A 5 kHz servo loop reads the sensors, computes control forces, and outputs current commands to the amplifiers. The dynamics of the master's induced motion pathway were identified via successive isolation, and the resulting model was tested in a position-force controller with cancellation of induced master motion.

A. Modeling Induced Master Motion

After a comprehensive evaluation of its dynamics under various conditions, our user-master system was found to exhibit a higher-order, nonlinear response that required successive isolation. A step-by-step account of the identification process is provided in [31], and here we present an overview of the final model. The master's linear current amplifier behaves almost ideally, giving $F_f' = F_f$, and the mechanical system is well-approximated by the nonlinear lumped-parameter model shown in Fig. 10. Motor, drum, and handle movements are mapped to translation of the user's hand by the unitless motor-to-drum gear ratio, $\rho = 15$, and the distance from the drum axis to the handle endpoint, $h = 0.15$ m. Both the motor and the drum exhibit significant Coulomb friction, and the cables behave like a simple spring and damper. Modeling the spring force of the joystick's linkage, F_{κ_l}, requires the nonlinear hysteretic description developed in [31]. All of the model's parameters, including the linkage's average effective stiffness, $\bar{k}_l$, are provided in Table I, and its basic equations of motion follow.

$$
\begin{aligned}
m_m\ddot{x}_m &= b_c(\dot{x}_d - \dot{x}_m) + k_c(x_d - x_m) + C_m + F_f \\
m_d\ddot{x}_d &= b_c(\dot{x}_m - \dot{x}_d) + k_c(x_m - x_d) - b_d\dot{x}_d - F_{\kappa_l} + C_d \\
m_h\ddot{x}_h &= F_{\kappa_l} - b_u\dot{x}_h - k_u x_h - q_u x_h^5
\end{aligned}
$$

$$
C_m = \begin{cases} -c_m & \text{if } \dot{x}_m > 0 \\ 0 & \text{if } \dot{x}_m = 0 \\ +c_m & \text{if } \dot{x}_m < 0 \end{cases}
\qquad
C_d = \begin{cases} -c_d & \text{if } \dot{x}_d > 0 \\ 0 & \text{if } \dot{x}_d = 0 \\ +c_d & \text{if } \dot{x}_d < 0 \end{cases}
$$

A linear stiffness model was found to adequately describe the user's behavior in the tested high-frequency range for moderate grip force values. Following the arguments of Section VI, we limit large deflections at DC by adopting a combined linear and quintic user stiffness model. The user's quintic stiffness, q_u, was tuned to allow only two millimeters of deflection at maximum feedback force. This user model thereby avoids overestimation of induced master motion at steady state, enabling the full model to capture the high-frequency, low-magnitude resonance that destabilizes teleoperation. The ETFE of the complete user-master system can be seen in Fig. 11, along with the ETFE of the overall model. The two match well, deviating only slightly in the low-frequency region. Although this model did not incorporate variations in the user's hand impedance during an interaction, it could easily be extended to do so in future work.

With all of its parameters identified, we tested the dynamic model's ability to predict the master's time response during haptic interactions. Several pre-recorded impact forces were

TABLE I

IDENTIFIED MASTER MODEL PARAMETERS.

Parameter	Value	Parameter	Value
k_u	40 N/m	m_d	0.0075 kg
q_u	3.125e+13 N/m^5	c_d	0.01 N
b_u	23 Ns/m	k_c	39500 N/m
m_h	0.014 kg	b_c	3.6 Ns/m
$\bar{k}_l$	3950 N/m	m_m	0.01075 kg
b_d	0.02 Ns/m	c_m	0.0144 N

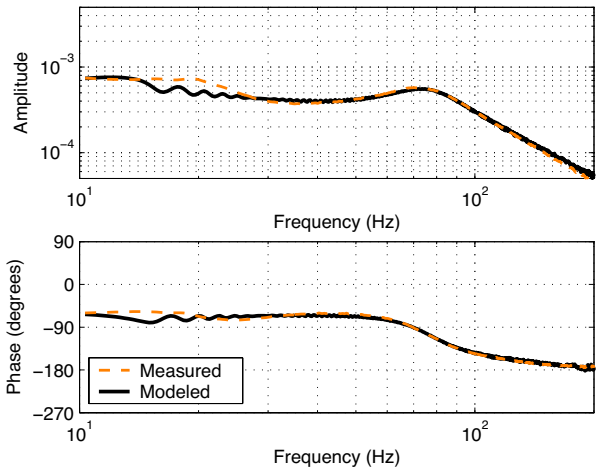

Fig. 11. When held by a user, the system exhibits a well-damped resonance at 70 Hz, in which the handle vibrates against the flesh of the user's hand.

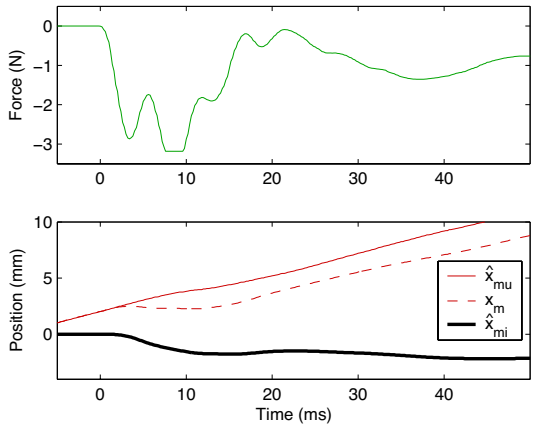

Fig. 12. The full model accurately predicts induced master motion during open-loop display of a pre-recorded force profile, providing a smooth estimate of user intention, $\hat{x}_{mu}$

displayed to a user via open-loop output. During these tests, the user held the handle of the master device, moving it forward as though tapping on a remote environment. The force profile was displayed when the user crossed a position threshold, and the resulting master motion, x_m, was recorded. The model was subjected to the same feedback force, F_f, and its prediction of induced master motion, $\hat{x}_{mi}$, was recorded. The cancellation approach's estimate of intended user motion was formulated for each of the tests as

$$\hat{x}_{mu} = x_m - \hat{x}_{mi}. \tag{8}$$

Open-loop testing indicates that the model adeptly captures the system's transient response to force feedback; results from a sample test are shown in Fig. 12. The induced motion prediction matches the shape and magnitude of the master's observed deviations for a range of force profiles, feedback gains, and incoming velocities. The resulting estimates of intended motion are smooth, nearly devoid of evidence of the applied force transient, supporting our assumption of superposition. The model's ability to estimate induced master motion during open-loop force display bodes well for its use in a closed-loop controller.

B. Canceling Induced Master Motion

The one-degree-of-freedom telerobotic system in Fig. 9 was used to test the cancellation approach with the identified model. Position-force control was implemented on the system, using proportional and derivative feedback on the slave. The full nonlinear master model was simulated in real time using forward Euler integration with a time step of 40 μs. The performance of this simple teleoperator was tested with and without cancellation, setting the force-feedback gain, λ, to various values, and keeping the position scale, μ, at unity. In these tests, the user tapped repeatedly on the environment, as though trying to explore its surface.

Fig. 13 shows a single representative contact for each of the eight testing conditions, illustrating the saturated force feedback signal, F_f, and commanded slave position, x_c. The bottom row of figures, which include cancellation, also show the measured master position, x_m, and the model's estimate of induced master motion, $\hat{x}_{mi}$. As seen in the first column of Fig. 13, contact with the environment at $\lambda = 1$ produces nearly identical behavior with and without cancellation. The force transients decay in about 50 ms, inducing only a small amount of high-frequency master motion. Although stable, this configuration does not provide the user with significant force cues.

When the feedback gain in increased to $\lambda = 3$, as shown in the second column of Fig. 13, the two controllers behave very differently. Without cancellation, the master experiences significant induced motion and the contact transient is prolonged to over 100 ms. The user experiences this effect as a slight buzzing on impact, which is completely removed by cancellation. The compensated system accurately predicts the induced master motion and prevents it from contaminating the slave's position command. By $\lambda = 6$, contact without cancellation creates highly oscillatory force feedback, as the slave makes and breaks contact with the environment several times. Adding cancellation provides a smooth estimate of the user's intended path for the slave, enabling stable contact under amplified force feedback. Increasing the gain even further, to $\lambda = 10$, brings about contact instability in the uncompensated system. The violent shaking of the master mechanism is prevented by including cancellation in the controller, keeping the force's settling time at approximately fifty milliseconds. As hoped, cancellation enables the user to receive amplified environment force feedback that is not distorted by the dynamics of the telerobotic system's internal control loop.

IX. Conclusions

Force-reflecting teleoperation has historically been plagued by contact instability, preventing the use of high feedback gains and leaving the user with faint haptic cues. This phenomenon can be traced to the dynamics of the master device, which must simultaneously measure the user's position command and apply force feedback. The position-force architecture inadvertently creates an internal controller loop, as force feedback induces motion of the master mechanism that is not intended as a position command. Large forward and feedback gains allow high-frequency oscillations to resonate in this internal controller loop, prolonging contact transients and ultimately causing system instability.

The controller's destabilizing inner loop can be severed by removing induced master motion from the slave's position command. The relationship between feedback force and master motion can be characterized by careful examination of device dynamics. The resulting model is simulated in real time during telerobotic interactions, and its output is subtracted from the measured master position to provide an estimate of user intention. We demonstrated this strategy on a one-dof master, building a nonlinear sixth-order model by isolating its successive elements and applying standard system identification techniques. The resulting model, which includes Coulomb and viscous friction, a novel nonlinear hysteretic linkage stiffness, and nonlinear skin stiffness, successfully captures the transient response of the system as held by a user.

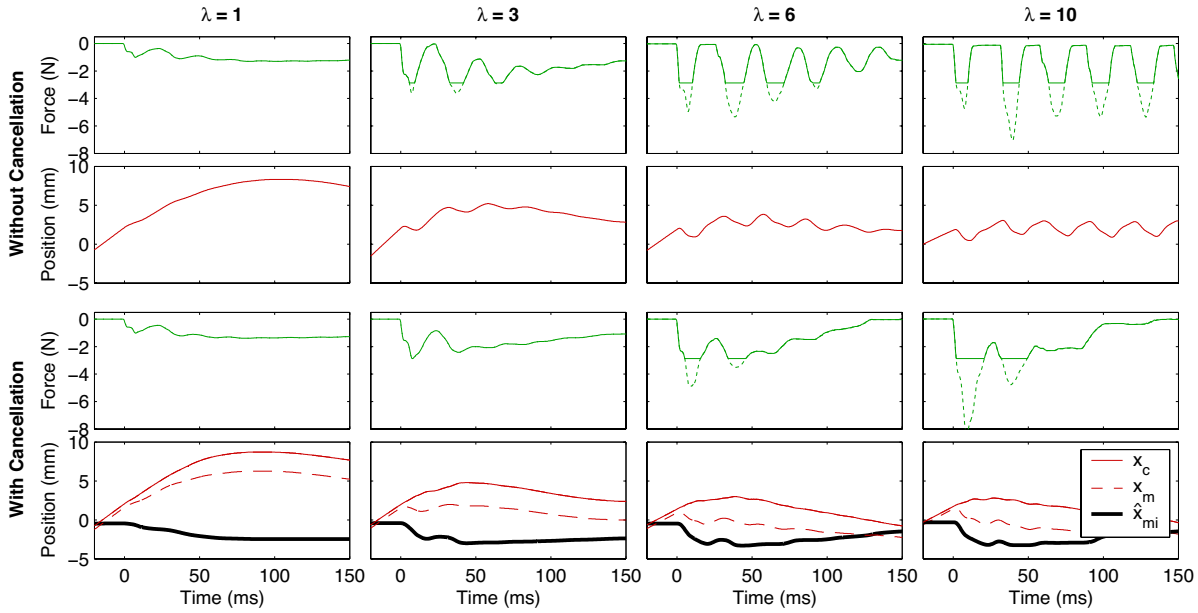

Fig. 13. Force feedback, F_f, and slave position command, x_c, with and without cancellation for a range of λ values, keeping $\mu = 1$. Contacts are stabilized by canceling induced master motion from the measured master position, x_m, using the model's real-time estimate, $\hat{x}_{mi}$.

Model-based cancellation was found to stabilize contact on the one-dof telerobotic testbed, preventing the violent oscillations that traditionally occur at high force reflection gains. Our approach attenuates the control loop's induced motion pathway and allows the system to provide stronger, more authentic force feedback. The model need not be perfect to provide these substantial benefits; its ability to describe the behavior of the master in the high-frequency region of the oscillations determines the performance improvements achieved. Our system enabled stable tapping up to a feedback gain of 15 with approximately constant transient decay time.

While anecdotal evidence suggests that these higher feedback gains provide a crisper feel to the user, we look forward to testing the cancellation approach in real teleoperative tasks. Future work will explore the importance of changes in the user's grip force, employing a grip force sensor to adjust the user's dynamic influence in real time. At present, our system cannot determine how the user is holding the handle, and a light grip can change the induced motion dynamics and interfere with cancellation. User parameters could also be characterized online, reducing the need for extensive offline tests. Finally, this strategy will be added to each joint of a multi-dof telerobotic system and tested during realistic operation to determine its effect on user experience.

The perspective of induced master motion also informs the process of master mechanism design. All impedance-type devices will allow some level of induced motion, so care should be taken to consider these dynamics. Generally, minimizing compliance in the device transmission will limit the induced motor motion pathway and provide better performance. Interestingly, this treatment of the master system also highlights the dynamic transmission of the force applied by the motor to the force experienced by the user at the handle. Having a full system model could enable the controller to adjust the feedback signal and counteract intervening transmission dynamics. We hope that this process of modeling and canceling induced master motion will enable future teleoperators to portray haptic interactions more authentically, allowing the user to telerobotically feel the full spectrum of forces that is available during real interactions.

APPENDIX

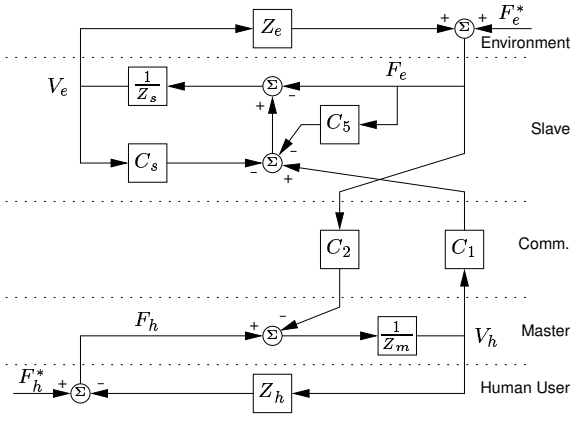

Fig. 14. Cancellation of induced master motion is implemented via C_5 in the general architecture for teleoperation.

Cancellation of induced master motion can also be understood by formulating it in teleoperation's four-channel architecture, which was first presented by Lawrence [13] and expanded by Hashtrudi-Zaad and Salcudean [33]. Such formulation requires three additional assumptions. First, linear models are used for the human, master, slave, and environment. Second, an impedance causality is assigned to both the human and environment. And lastly, human forces and

motor forces are collocated, acting on the master with the same transfer function. Nevertheless, this architecture provides a useful perspective on the cancellation approach. A position-force controller with cancellation is illustrated in Fig. 14 using the common nomenclature for the various subsystem blocks. Elements that are not typically used in position-force control are not illustrated, i.e. $C_3 = C_4 = C_6 = C_m = 0$. The values for the remaining elements are

$$C_1 = \mu(b + k/s) \quad C_s = b + k/s$$
$$C_2 = \lambda \quad C_5 = -\lambda\mu\frac{(b+k/s)}{\hat{Z}_m + \hat{Z}_h}$$

where b and k are slave controller gains and s is the Laplace operator. Cancellation of induced master motion is embodied in the C_5 element, which is usually regarded as a local force control loop on the slave. It works to prevent the environmental contact force, here F_e, from contributing to the slave's control force through the passive dynamics of the master and user. If the master and human models ($\hat{Z}_m$ and $\hat{Z}_h$) are accurate, the net force applied to the slave via C_1, C_s, and C_5 will represent only the user's active influence on the master, F_h^*.

REFERENCES

[1] Goertz, R. C., 1952. "Fundamentals of general-purpose remote manipulators". Nucleonics, **10** (11) Nov. , pp. 36–45.

[2] Goertz, R. C., 1954. "Electronically controlled manipulator". Nucleonics, **12** (11) Nov. , pp. 46–47.

[3] LaMotte, R. H., 2000. "Softness discrimination with a tool". Journal of Neurophysiology, **83** (4) Apr. , pp. 1777–1786.

[4] Kontarinis, D. A., and Howe, R. D., 1995. "Tactile display of vibratory information in teleoperation and virtual environments". Presence: Teleoperators and Virtual Environments, **4** (4) , pp. 387–402.

[5] Okamura, A. M., Dennerlein, J. T., and Howe, R. D., 1998. "Vibration feedback models for virtual environments". In Proc. IEEE Int. Conf. on Robotics and Automation, pp. 674–679.

[6] Okamura, A. M., Cutkosky, M. R., and Dennerlein, J. T., 2001. "Reality-based models for vibration feedback in virtual environments". IEEE/ASME Transactions on Mechatronics, **6** (3) Sept. , pp. 245–252.

[7] Kuchenbecker, K. J., Fiene, J., and Niemeyer, G., 2005. "Event-based haptics and acceleration matching: Portraying and assessing the realism of contact". In Proc. IEEE World Haptics Conference.

[8] Colgate, J. E., 1993. "Robust impedance shaping telemanipulation". IEEE Transactions on Robotics and Automation, **9** (4) Aug. , pp. 374–384.

[9] Daniel, R. W., and McAree, P. R., 1998. "Fundamental limits of performance for force reflecting teleoperation". Int. Journal of Robotics Research, **17** (8) Aug. , pp. 811–830.

[10] Sitti, M., and Hashimoto, H., 2003. "Teleoperated touch feedback from the surfaces at the nanoscale: Modeling and experiments". IEEE/ASME Transactions on Mechatronics, **8** (2) June , pp. 287–298.

[11] Rassweiler, J., Binder, J., and Frede, T., 2001. "Robotic and telesurgery: will they change our future". Current Opinion in Urology, **11** (3) May , pp. 309–320.

[12] Goldfarb, M., 1998. "Dimensional analysis and selective distortion in scaled bilateral telemanipulation". In Proc. IEEE Int. Conf. on Robotics and Automation, pp. 1609–1614.

[13] Lawrence, D. A., 1993. "Stability and transparency in bilateral teleoperation". IEEE Transactions on Robotics and Automation, **9** (5) Oct. , pp. 624–637.

[14] Fite, K. B., Speich, J. E., and Goldfarb, M., 2001. "Transparency and stability robustness in two-channel bilateral telemanipulation". *Journal of Dynamic Systems, Measurement, and Control,* **123** Sept. , pp. 400–407.

[15] Hannaford, B., and Anderson, R., 1988. "Experimental and simulation studies of hard contact in force reflecting teleoperation". In Proc. IEEE Int. Conf. on Robotics and Automation, vol. 1, pp. 584–589.

[16] Bu, Y., Daniel, R. W., and McAree, P. R., 1996. "Stability analysis of force reflecting telerobotic systems". In Proc. IEEE Int. Conf. on Intelligent Robots and Systems, vol. 3, pp. 1374–1379.

[17] Hannaford, B., 1989. "A design framework for teleoperators with kinesthetic feedback". IEEE Transactions on Robotics and Automation, **5** (4) Aug. , pp. 426–434.

[18] Kuchenbecker, K. J., and Niemeyer, G., 2004. "Canceling induced master motion in force-reflecting teleoperation". In Proc. ASME Int. Mechanical Engineering Congress and Exposition, vol. 2, 60049.

[19] Yokokohji, Y., and Yoshikawa, T., 1994. "Bilateral control of master-slave manipulators for ideal kinesthetic coupling - formulation and experiments". IEEE Transactions on Robotics and Automation, **10** (5) Oct. , pp. 605–620.

[20] Lee, H.-K., and Chung, M. J., 1998. "Adaptive controller of a master-slave system for transparent teleoperation". Journal of Robotic Systems, **15** (8) , pp. 465–475.

[21] Gillespie, R. B., Hasser, C., and Tang, P., 1999. "Cancellation of feedthrough dynamics using a force-reflecting joystick". In Proc. ASME Dynamic Systems and Control Division, pp. 319–326.

[22] Sirouspour, M. R., and Salcudean, S. E., 2003. "Suppressing operator-induced oscillations in manual control systems with movable bases". IEEE Transactions on Control Systems Technology, **11** (4) July .

[23] Hogan, N., 1989. "Controlling impedance at the man / machine interface". In Proc. IEEE Int. Conf. on Robotics and Automation, vol. 3, pp. 1626–1631.

[24] Kearney, R. E., and Hunter, I. W., 1990. "System identification of human joint dynamics". Critical Reviews in Biomedical Engineering, **18** (1) , pp. 55–87.

[25] Hasser, C. J., and Cutkosky, M. R., 2002. "System identification of the human grasping a haptic knob". In Proc. IEEE Haptics Symposium, pp. 171–180.

[26] Kuchenbecker, K. J., Park, J. G., and Niemeyer, G., 2003. "Characterizing the human wrist for improved haptic interaction". In Proc. ASME Int. Mechanical Engineering Congress and Exposition, vol. 2, 42017.

[27] Burström, L., 1997. "The influence of biodynamic factors on the mechanical impedance of the hand and arm". Int. Archives of Occupational and Environmental Health, **69** (6) June , pp. 437–446.

[28] Rancourt, D., and Hogan, N., 2001. "Stability in force-production tasks". Journal of Motor Behavior, **33** (2) , pp. 193–204.

[29] Osu, R., and Gomi, H., 1999. "Multijoint muscle regulation mechanisms examined by measured human arm stiffness and emg signals". Journal of Neurophysiology, **81** (4) , pp. 1458–1468.

[30] Gribble, P. L., Mullin, L. I., Cothros, N., and Mattar, A., 2003. "Role of cocontraction in arm movement accuracy". Journal of Neurophysiology, **89** (5) May , pp. 2396–2405.

[31] Kuchenbecker, K. J., and Niemeyer, G., 2005. "Modeling induced master motion in force-reflecting teleoperation". In Proc. IEEE Int. Conf. on Robotics and Automation.

[32] Diolaiti, N., Niemeyer, G., Barbagli, F., Salisbury, J. K., and Melchiorri, C., 2005. "The effect of quantization and coulomb friction on the stability of haptic rendering". In Proc. IEEE World Haptics Conference.

[33] Hashtrudi-Zaad, K., and Salcudean, S. E., 2001. "Analysis of control architectures for teleoperation systems with impedance/ admittance master and slave manipulators". Int. Journal of Robotics Research, **20** (6) June , pp. 419–445.